In-train forces from energy-efficient driving strategies

P. Zhou[a], **P. Pudney**[b] **and P. Howlett** [b]

[a]*School of Information Technology and Mathematical Sciences, University of South Australia, Mawson Lakes, South Australia*
[b]*Scheduling and Control Group, Barbara Hardy Institute, University of South Australia, Mawson Lakes, South Australia*
Email: Peng.Zhou@unisa.edu.au

Abstract: For many years the Scheduling and Control Group at the University of South Australia has been developing systems that provide driving advice to train drivers to help them stay on time and minimise energy use. These control strategies minimise the mechanical work done by the traction system, which in practice gives savings of 10–20% in the diesel fuel or electrical energy used to power the train.

These energy-efficient driving strategies require the driver to switch between maximum power and coasting and between coasting and braking. On long, heavy trains, control transitions combined with changes of gradient can cause the connections between wagons to change between tension and compression. In extreme cases, the forces between wagons can be high enough to break a coupler. Although energy-efficient driving is designed to minimise total energy input it is still possible that excess energy will contribute to unacceptable in-train forces at some critical locations.

In this paper we describe different models that can be used to estimate in-train forces on long trains, and we use the most realistic of these models to show that control transitions that may occur with energy-efficient driving do not result in excessive in-train forces.

Keywords: Energy-efficient driving, optimal control, in-train forces.

1 INTRODUCTION

Rail operators are increasingly turning to technology to help drivers control their trains more efficiently. Driver Advice Systems are in-cab systems that monitor the progress of a train journey and provide advice on how the train should be driven in order to meet the timetable with minimum energy use. Driver Advice Systems are being installed on passenger trains and freight trains around the world, and are helping drivers achieve improved timekeeping and energy savings of 10–20%. However, these systems do not replace the driver—the driver is still vital for ensuring that the train is driven safely, and smoothly. The train models used to calculate efficient driving strategies do not necessarily take into account the full train dynamics. Even though Driver Advice Systems have been successfully deployed on long, heavy trains—up to 2500 m long and 17000 tonnes—there is still concern in the rail industry that following the advice may sometimes cause excessive forces in the couplers between wagons and ultimately lead to the train breaking.

Driver Advice Systems typically use a single body model of train dynamics to calculate an optimal driving strategy (Howlett et al., 1994; Khmelnitsky, 2000; Howlett et al., 2009). Our Energymiser system uses GPS receivers to monitor the position and speed of a train, and specialised software to calculate the optimal sequence of control modes. The style of driving advised by Energymiser is familiar to many drivers, and often referred to as *momentum driving*. The key idea is to use the momentum of the train to minimise fluctuations in speed. Full power is applied to get the train up to speed and prior to steep inclines. Partial power or braking is used to hold a constant speed. Power is reduced for steep declines and before braking. The speed of the train is allowed to fall before a steep decline or before a speed restriction so that less braking is required. Drivers using Energymiser save energy by holding at speeds less than the speed limit, and reducing power earlier than they would without Energymiser. Instead of arriving early, the train will arrive on time with reduced energy use.

Energymiser provides general advice on how fast the train should be travelling and where power can be reduced. If Energymiser advises a change of driving mode, to Coast or to Drive, the driver should make the transition as they normally would. On long heavy trains, drivers know that in practice they must adjust the traction and braking forces gradually to avoid excessive in-train forces.

There are two key scenarios where Energymiser advice could be different to what a driver would normally do and where there is potential for generating large in-train forces:

- a Drive–Brake–Drive sequence that may occur if a train is driving up a steep incline, brakes to slow to a restrictive speed limit, then resumes driving with maximum power on the steep incline
- a Drive–Coast transition before the crest of a hill.

The first scenario will not actually be advised by Energymiser—there will always be a Coast mode between Drive and Brake. But we will analyse it anyway, as an extreme case; the Brake–Drive transition can be advised.

2 MODELLING IN-TRAIN FORCES

For the purposes of modelling the dominant longitudinal forces within the train we will consider a model where each locomotive or wagon is treated as a single body. Complicated multi-body models are used for more detailed studies of wagon motion when analysing, for example, derailments, but are not necessary for studying the dominant longitudinal dynamics forces.

We will consider a train where the first vehicle is a locomotive and all remaining vehicles are wagons, and where the locomotive provides all traction and braking forces, since this will give the greatest in-train forces. Figure 1 shows the relevant forces on vehicle i. They are: F_i, the force from the coupler at the front of the vehicle; G_i, the gradient forces on the vehicle; R_i, the resistance forces on the vehicle; and F_{i+1}, the force from the coupler at the rear of the vehicle.

The distance along the route of vehicle i is x_i; the speed of vehicle i is v_i. The force F_1 is the controlled traction or braking force of the locomotive.

The black block between vehicles represents a coupler system, which may include springs and dampers.

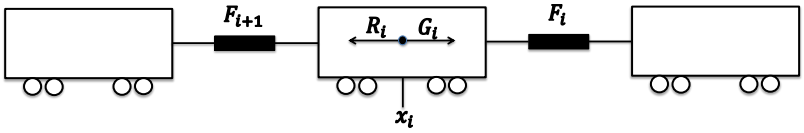

Figure 1. Forces acting on a vehicle.

The motion of the vehicles is described by the equations

$$\frac{dx_1}{dt} = v_1 \tag{1}$$

$$\frac{dx_i}{dt} = v_i \qquad i \in \{2, \ldots, n\} \tag{2}$$

$$m_i \frac{dv_i}{dt} = F_i - F_{i+1} - R_i + G_i \qquad i \in \{1, 2, \ldots, n-1\} \tag{3}$$

$$m_n \frac{dv_n}{dt} = F_n - R_n + G_n \tag{4}$$

where $R_i = R(v_i)$ and $G_i = G(x_i)$.

The coupler between vehicles $i-1$ and i exerts a force $-F_i$ on vehicle $i-1$ and an opposite force F_i on vehicle i. The force F_i depends on the behaviour of the coupler. Gruber and Bayoumi (1982) and Ansari and Esmailzadeh (2009) assume a simple spring and damper with constant spring coefficient k_s and constant damper coefficient k_d; the coupler force is

$$F(\xi, v) = k_\mathrm{s}\xi - k_\mathrm{d}v$$

where ξ is the extension of the coupler and v is the rate of change of the extension. The extension of the coupler between vehicles i and $i+1$ is $\xi_i = x_i - x_{i+1} - l_i$, where l_i is the nominal distance between vehicles i and $i+1$.

Astolfi and Menini (2002) and Yang and Sun (1999, 2001) use more realistic nonlinear spring models, where the force increases nonlinearly with the extension of the spring:

$$F(\xi, v) = k_\mathrm{s}(1 + \varepsilon\xi^2)\xi - k_\mathrm{d}v$$

where ε is the coefficient of nonlinearity. Zhuan and Xia (2006) use a piecewise linear spring model, but without damping.

Figures 2(a) and 2(b) show how force F varies with extension for the simple linear and non-linear spring models. The middle curve in each of these graphs indicates the response for $v = 0$, the lower curve indicates the response for $v > 0$ and the upper curve indicates the response for $v < 0$.

To be more realistic, we need to understand the details of the structure of vehicle couplers. Figure 3 shows a schematic diagram of a coupler unit, in various positions. There is one of these on each vehicle, with an essentially rigid joint between them connecting the red rods. The black rectangles represent fixed points on the vehicle. As the red rod moves right, it pushes on the yellow follower which compresses the spring and at the same time pushes the purple wedges outwards. The force of the wedges against the sides of the cylinder opposes the motion. When the red rod moves left, it moves the spring housing which in turn compresses the spring and again pushes the wedges outwards. The action of the wedges produces a force that opposes the motion when the spring is compressing, and when the spring is extending. The resulting graph of (extension, force) is shown in Figure 2(c):

- if $\xi > 0$ and $v > 0$ (the coupler is extended and extending), the springs and wedges each oppose the motion and the force is given by the lower curve in the bottom right quadrant of the graph
- if $\xi > 0$ and $v < 0$ the springs assist the motion but the wedges oppose the motion, and the force is given by the upper curve in the bottom right quadrant of the graph

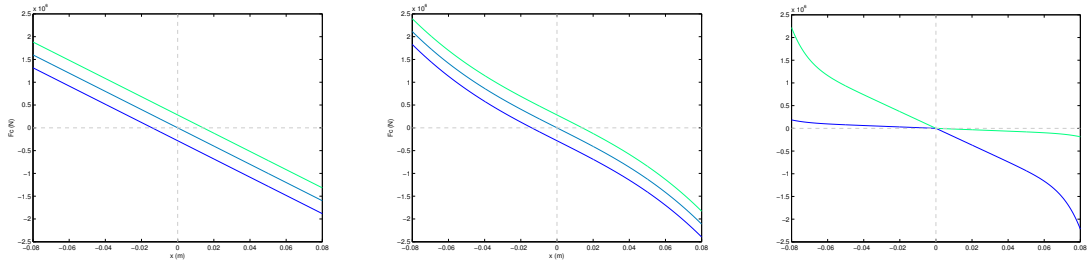

(a) Linear spring and damper. (b) Nonlinear spring and damper. (c) A more realistic coupler unit model.

Figure 2. Coupler force graphs.

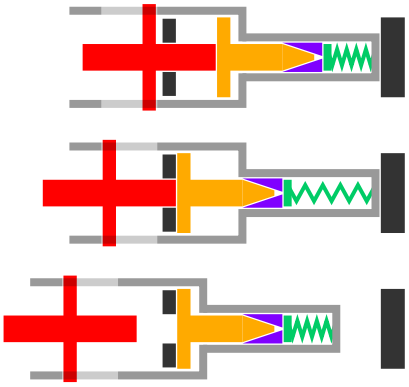

Figure 3. Fully compressed, at rest, and fully extended coupler units. The black boxes are fixed to the vehicle; the remaining parts can move.

- if $\xi < 0$ and $v < 0$ then the springs and wedges each oppose the motion and the force is given by the upper curve in the top left quadrant of the graph
- if $\xi < 0$ and $v > 0$ then the springs assist the motion but the wedges oppose the motion, and the force is given by the lower curve in the top left quadrant of the graph.

Cole (2006), Cantone and Durand (2011) and Wu et al. (2012) each use models with these characteristics; they differ only in their assumptions about how the force transitions between the loading curve (when the extension and velocity have the same sign and the spring is compressing) and the unloading curve (when the extension and velocity have different signs and the spring is extending).

The coupling between two wagons comprises two coupler units. We use

$$F(\xi, v) = 2k\left(\xi/2 + c(\xi/2)^9\right)$$

where the coefficients are $k = 20 \times 10^6\,\mathrm{kg\,s^{-2}}$ and $c = 3 \times 10^8$ when the spring is loading ($\xi > 0, v \geq \epsilon = 0.1\,\mathrm{m\,s^{-1}}$ or $\xi < 0, v \leq \epsilon = 0.1\,\mathrm{m\,s^{-1}}$). When the spring is unloading ($\xi > 0, v \leq \epsilon = 0.1\,\mathrm{m\,s^{-1}}$ or $\xi < 0, v \geq \epsilon = 0.1\,\mathrm{m\,s^{-1}}$) we use $k = 2 \times 10^6\,\mathrm{kg\,s^{-2}}$. When $-\epsilon < v < \epsilon$ we interpolate between the loading and unloading curves. All the other cases, $k = 20 \times 10^6\,\mathrm{kg\,s^{-2}}$. The coefficients were selected to approximate experimental data from Cole (2006).

3 Simulations

The following simulations show the effect of various control transitions on a train with a locomotive and 50 wagons. The locomotive has a mass of 300 tonnes, and each wagon has a mass of 100 tonnes. Each vehicle has a length of 20 m. The maximum locomotive power is 10.6 MN. The resistance force on each vehicle i is $R(v) = m_i(0.0005 + 0.00002v^2)$.

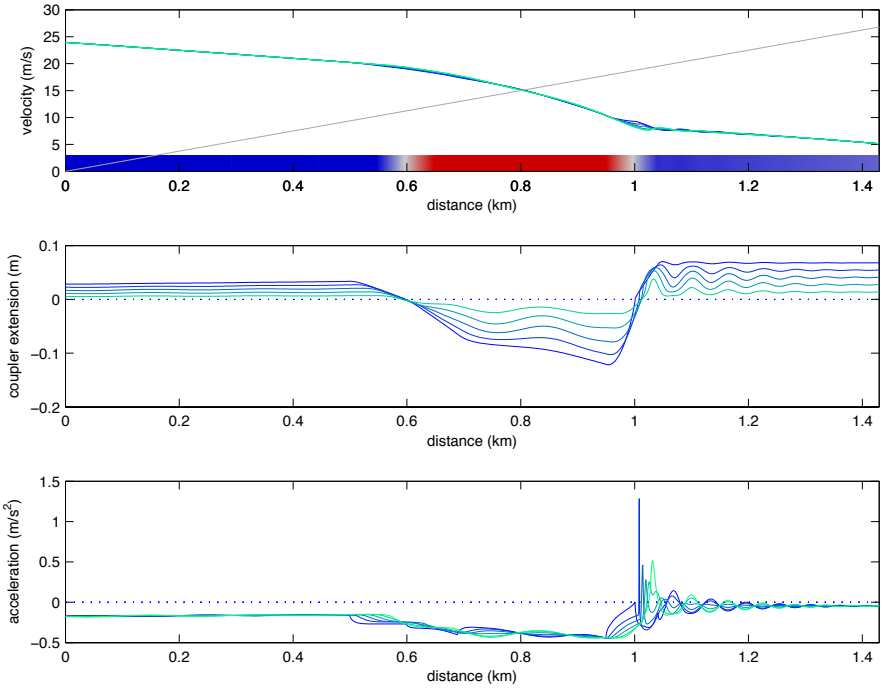

Figure 4. Drive – Brake – Drive on a steep incline. There is a spike in acceleration as the locomotive changes from Brake to Power, but it is less than 1.5 ms^{-2}. The magnitude of the spike reduces as the transition time between Brake and Power is increased from 10 seconds, and disappears at 13 seconds.

Each diagram has three graphs, showing the speed and acceleration of vehicles 1, 11, ..., 51, and the the coupler extension of couplers 1, 11, ..., 41. The colours of the curves graduate from blue at the front of the train to green at the rear of the train. The coloured band at the bottom of the speed graph indicates the control: blue indicates Drive, grey indicates Coast, red indicates Brake. The elevation profile is indicated as a grey line on the speed graph.

Figure 4 shows the effect of transitions from Drive to Brake to Drive while the train is on a steep incline. The transition duration is 10 seconds. The second change, from Brake back to Drive, causes larger accelerations than the first, but the spikes in acceleration are less than 1.5 ms^{-2}.

Figure 5 shows the effect of a transition from Drive to Coast well before the crest of a hill. The gradient is +0.015 before the crest, and -0.030 after the crest, with a realistic transition between these gradients.

Figure 6 shows the effect of a transition from Drive to Coast at the crest of a realistic hill, which is more like what drivers would do in practice.

4 Conclusions

The driving mode transitions advised by Driver Advice Systems such as Energymiser do not appear to cause abnormally high forces when the control is moved smoothly between modes, as is normal driving practice. In each of the scenarios examined, the coupler extensions were never significantly larger than when travelling at constant speed. A transition from full braking to full power caused the highest acceleration spikes, but these were less than 1.5 ms^{-2}, which is not excessive—Cole and Sun (2006) calculates typical accelerations of up to 4 ms^{-2}.

Acknowledgements

This research was supported under Australian Research Council's *Linkage Projects* funding scheme (project number LP110100136).

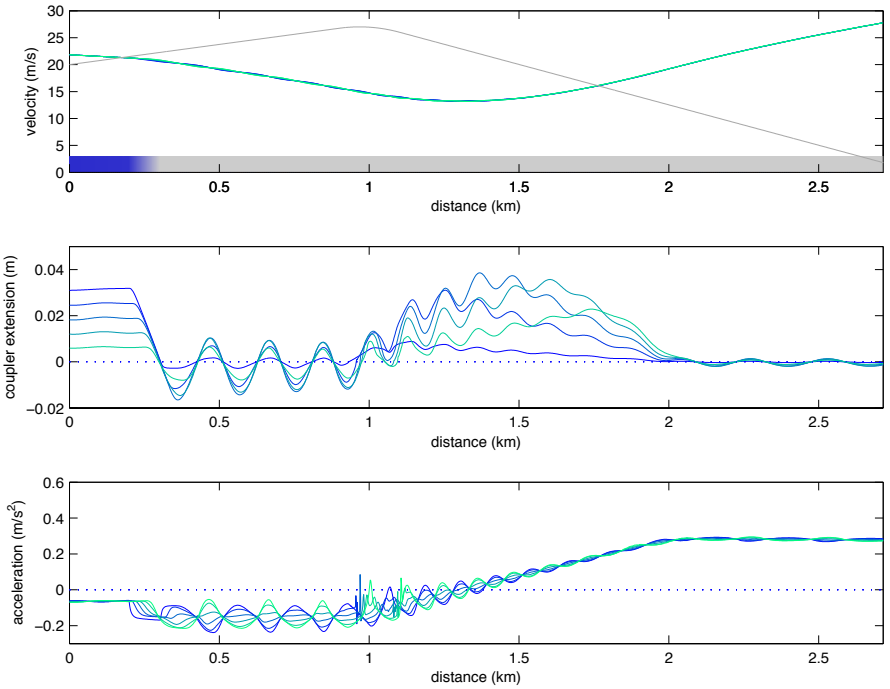

Figure 5. Early coasting over a crest. There are some small spikes in acceleration as vehicles move over the crest.

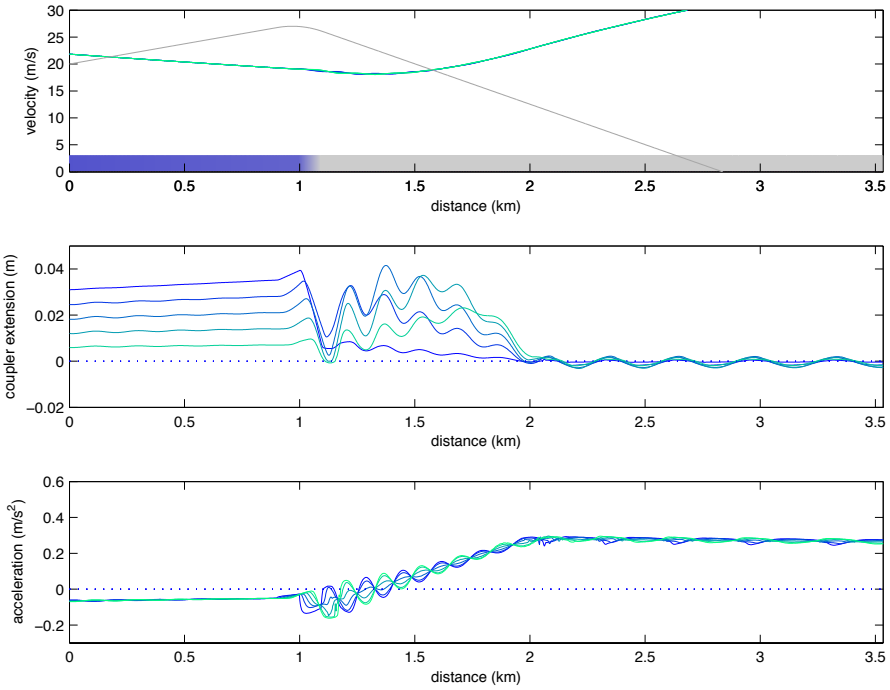

Figure 6. Late coasting over a crest. The accelerations are slightly smaller than when the train coasted earlier, and there are no spikes.

REFERENCES

Ansari, M. and E. Esmailzadeh (2009). Longitudinal dynamics of freight trains. *Heavy Vehicle Systems 16*, 102–131.

Astolfi, A. and L. Menini (2002, May). Input/output decoupling problems for high speed trains. *American Control Conference*.

Cantone, L. and T. Durand (2011, May). Longitudinal forces evaluation of sncf trains. *9th World Congress on Railway Research*.

Cole, C. (2006). *Handbook of railway vehicle dynamics*. CRC Press.

Cole, C. and Y. Q. Sun (2006). Simulated comparisons of wagon coupler systems in heavy haul trains. *Journal of Rail and Rapid Transit 220*(3), 247–255.

Gruber, P. and M. M. Bayoumi (1982). Suboptimal control strategies for multilocomotive powered trains. *Automatic Control 27*(3), 536–546.

Howlett, P., I. Milroy, and P. Pudney (1994). Energy–efficient train control. *Control Engineering Practice 2*(2), 193–200.

Howlett, P., P. Pudney, and X. Vu (2009). Local energy minimization in optimal train control. *Automatica 45*, 2692–2698.

Khmelnitsky, E. (2000). On an optimal control problem of train operation. *IEEE Transactions on Automatic Control 45*(7), 1257–1266.

Wu, Q., L. Shi-hui, W. Chong-feng, and M. Wei-hua (2012, Jun). Dynamics simulation models of coupler systems for freight locomotive. *Journal of Traffic and Transportation Engineering 12*(3), 37–43.

Yang, C. and Y.-P. Sun (2001). Mixed H_2/H_∞ cruise controller design for high speed train. *Journal of Control 74*(9), 905–920.

Yang, C.-D. and Y.-P. Sun (1999, June). Robust cruise control of high speed train with hardening/softening nonlinear coupler. *American Control Conference*.

Zhuan, X. and X. Xia (2006, July). Cruise control scheduling of heavy haul trains. *Control systems technology 14*(4), 757–766.